Chemosphere 297 (2022) 134073

Contents lists available at ScienceDirect

Chemosphere

journal homepage: www.elsevier.com/locate/chemosphere

Retention of sulfamethoxazole by cinnamon wood biochar and its efficacy of reducing bioavailability and plant uptake in soil

S. Keerthanan [a], Chamila Jayasinghe [b], Nanthi Bolan [c], Jorg Rinklebe [d], Meththika Vithanage [a,*]

[a] Ecosphere Resilience Research Center, Faculty of Applied Sciences, University of Sri Jayewardenepura, Nugegoda, 10250, Sri Lanka
[b] Department of Food Science and Technology, Faculty of Livestock, Fisheries and Nutrition, Wayamba University of Sri Lanka. Makandura, Gonawila, Sri Lanka
[c] School of Agriculture and Environment, The UWA Institute of Agriculture, The University of Western Australia, M079, Perth WA, 6009, Australia
[d] Soil- and Groundwater-Management, Institute of Soil Engineering, Waste- and Water Science, Faculty of Architecture und Civil Engineering, University of Wuppertal, Germany

HIGHLIGHTS

- Cinnamon wood biochar (CWBC) has a strong affinity (113 mg/g) for sulfamethoxazole (SUL).
- Adsorption capacity of soil and CWBC amendment towards SUL were 0.67 and 3.36 mg/g.
- Root and shoot of *Ipomoea aquatica* acquired 13.8 and 0.027 mg/kg of SUL.
- The plant accumulation of SUL was sensitive to the soil contamination level.
- The CWBC amendment reduced SUL accumulation in root by 30–60%, and shoot by 61–95%.

GRAPHICAL ABSTRACT

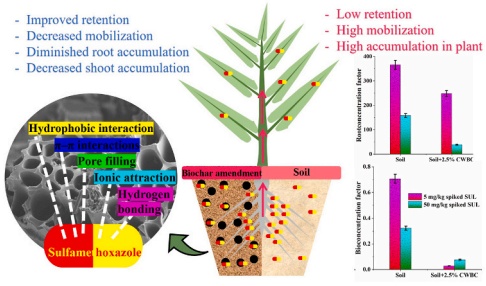

ARTICLE INFO

Handling Editor: Govarthanan Muthusamy

Keywords:
Antibiotics
Sulfonamide
Plant uptake
Remediation
Amendment

ABSTRACT

The objective of this research was to evaluate the efficacy of cinnamon wood biochar (CWBC) in adsorbing sulfamethoxazole (SUL), which alleviates bioavailability and plant uptake. Batch studies at various pH, contact times, and initial SUL loading were used to study SUL adsorption in CWBC, soil, and 2.5% CWBC amended soil. SUL mitigation from plant uptake were examined using *Ipomoea aquatica* at different SUL contamination levels in the soil. The kinetic results were described by pseudo-second-order with maximum adsorption capacities (Q_{max}) of 95.64 and 0.234 mg/g for pristine CWBC and amendment, respectively implying that chemical interactions are rate-determining stages. Hill and Toth's model described the isotherm data for pristine CWBC, soil and CWBC amended soil as Q_{max} of 113.44, 0.72, and 3.45 mg/g. Column data showed a great mobilization of SUL in loamy sand; however, when CWBC was added to the loamy sand, the mobilization was drastically reduced by 98.8%. The *Ipomoea aquatica* showed a great potential to SUL uptake and it depended on the contamination level; the SUL accumulation in plant was 9.6–13.8 and 19.1–48 mg/kg when soil was spiked with 5 and 50 mg/kg, respectively. The addition of 2.5% CWBC reduced root and shoot uptake by 30 and 95%, respectively in 5 mg/kg of SUL, whereas with 50 mg/kg of SUL, the root and shoot uptake was reduced by 60 and 61%, respectively. The current study suggested CWBC as a possible adsorbent that may be employed to reduce SUL bioavailability in environmental matrices.

* Corresponding author.
E-mail address: meththika@sjp.ac.lk (M. Vithanage).

https://doi.org/10.1016/j.chemosphere.2022.134073
Received 1 November 2021; Received in revised form 16 February 2022; Accepted 19 February 2022
Available online 25 February 2022

1. Introduction

Antibiotics are a critical emerging contaminant among various pharmaceutical and personal care products (PPCPs), accumulated in the environment through excessive use and haphazard disposal. Once the antibiotics are consumed, 30–90% of them are excreted out via urine and feces, in the form of either metabolites or parental forms (Sivagami et al., 2020). As a result, the antibiotic residues exponentially increase in the environmental matrices, including water, soil, and plants (Azanu et al., 2018; Liu et al., 2020; Sun et al., 2019). The presence of antibiotic residues in the environment causes deleterious effects on humans and non-target organisms and creates antibiotic-resistant microbes in the environment.

Among the number of antibiotics, sulfamethoxazole (SUL) is a commonly and globally prescribed sulfonamides group medicine for human and veterinary animals. About 80–90% of SUL is excreted along with urine within 24 h of oral administration, as SUL and acetylated SUL form (Scholar, 2007), which raises the toxicity in the environment matrices. SUL was recently found in surface water at 934 ng/L in Sri Lanka (Guruge et al., 2019) and in the soil at 1.4 g/kg in China (Liu et al., 2020). A previous study by Christou et al. (2017) reported SUL concentration in the soil as 0.38–0.98 μg/kg irrigated with municipal wastewater treatment effluent containing 25–55 ng/L of SUL. It has been observed that various crops can take up SUL residues and enter into the animals and humans via the food chain. The consumption of SUL per day was calculated as <0.1, 0.77, and 9.5 μg from drinking water, fish meat, and crops, respectively (Straub, 2016). This indirect human exposure of SUL was lesser than the daily permissible limit of 10 mg/day (Straub, 2016). However, the acute toxic level (EC_{50}) of SUL for invertebrates and algae was at a range of 26.8–2400 μg/L (Ferrari et al., 2004) and fishes and invertebrates were at a range of 15.5–35.4 mg/L (Isidori et al., 2005). Although indirect SUL exposure poses no health risk to humans, accumulation in fish and birds, and environmental SUL exposure can result in the development of SUL resistance genes in microbes, leading to negative consequences for humans and non-target species. Therefore, the removal and retaining of SUL from the contaminated water and soil is urgently needed, ultimately reducing the plant uptake.

Principally, the contaminants in soil pore water can be taken up by the root of the plants and accumulated in the different parts of the plants. Accordingly, in order to reduce the plant uptake, the contaminants in the pore water should be immobilized in the soil system. This can be achieved by amendments with carbonaceous materials such as activated carbon and biochar. However, biochar is an alternative material for activated carbon, due to its less energy requirement and high production yield of biochar (Jayawardhana et al., 2021a; Panwar et al., 2019). It can be primarily produced from various biomass sources at different pyrolysis conditions. Moreover, biochar can be a byproduct of bioenergy producing industries. Various studies suggested the potential of biochar in removing inorganic and organic contaminants from wastewater (Ashiq et al., 2019; Hassan et al., 2020; Shan et al., 2020; Zhang et al., 2019). Ashiq et al. (2019) reported that the maximum removal affinity of municipal solid waste biochar towards ciprofloxacin antibiotics as 168 mg/g (Ashiq et al., 2019). Moreover, the soil biochar amendment not only enhances the retention of contaminants such as PPCPs, polyaromatic hydrocarbons, and heavy metals (Cao et al., 2016; Keerthanan et al., 2021; Uchimiya et al., 2010) but also improves soil fertility by providing some of the essential nutrients required for the plant growth (He et al., 2020; Plaimart et al., 2021; Zhang et al., 2021).

Recent studies investigated SUL uptake by plants such as cucumber and water spinach grown in hydroponic solutions, and the plants presented a hyperaccumulation towards SUL (Kurade et al., 2019; Sun et al., 2018). The low distribution coefficient between soil and soil-pore water (Li et al., 2020) increases the bioavailability of SUL in soil. It is essential to decrease the available fraction of SUL in the soil to reduce plant uptake ultimately. However, the effects of gasified biochar in lowering the bioavailability of SUL in environmental matrices and a mechanistic understanding of the interactions at a molecular level are lacking in current knowledge. Furthermore, the chemical behavior of SUL in soil with and without biochar is present, the plant uptake behavior of SUL, and its mitigation from plant uptake using biochar is still unclear in the literature. Therefore, the present study aimed: (1) to assess the removal of SUL from aqueous media using cinnamon wood biochar (CWBC) through batch experiments and understand the mechanistic insight; (2) to evaluate the immobilization and mobilization of SUL in soil and CWBC amended soil; (3) to assess the influence of CWBC in limiting the bioavailable fraction of SUL for plant uptake in soil; (4) to evaluate the bioaccumulation and translocation of SUL in *Ipomoea aquatica*.

2. Material and methodology

2.1. Chemicals

Analytical standard grade sulfamethoxazole (sigma Aldrich, Switzerland) and all chemicals, including simeton as an internal standard (Chem service, USA), liquid chromatography-mass spectroscopy/mass spectroscopy (LC-MS/MS) grade acetonitrile (sigma Aldrich), high performance liquid-chromatography (HPLC) grade methanol (sigma Aldrich), formic acid (Merck, Finland), potassium dihydrogen phosphate (Fluka), Fourier-transform infrared spectroscopy (FTIR) grade potassium bromide (sigma Aldrich), analytical grade acetone and hexane (Merck, India), and hydrochloric acid and sodium hydroxide (sigma Aldrich) used to adjust the pH were purchased. The solid-phase extraction (SPE) HLB (hydrophilic-lipophilic balanced) cartridges (60 mg/3 mL) were purchased from Supelco sigma Aldrich.

2.2. Biochar, soil collection and amendment preparation

The byproduct of cinnamon wood biochar (CWBC) was collected from the bioenergy generating industry in Sri Lanka, where the cinnamon wood waste undergoes gasification at 700 °C. Afterward, CWBC was crushed, ground, and passed through a 250 μm sieve. The soil in 0–15 cm depth at hot and humid environment was collected in a model forest patch of the University of Sri Jayewardenepura, Sri Lanka (6°51′15.4″N 79°54′12.8″E), with no antibiotic contamination and the soil was characterized as a loamy sand (Keerthanan et al., 2021). The collected soil was dried under sunlight for 4 h and sieved through a 2 mm mesh. The CWBC amended soil was prepared thoroughly, mixing 2.5% of CWBC with the soil and equilibrating for 8 weeks at 70% field capacity moisture content. Finally, the CWBC, soil, and CWBC amended soil was stored in separate plastic bags until the experiments began.

2.3. Characterization of CWBC

The pH and electrical conductivity (EC) of CWBC, soil, and CWBC amended soil were determined by a pH meter (AD1030, Adwa, Romania) and a conductivity meter (EUTECH Con 450, Thermo scientific), respectively at 1:10 (w/v) ratio of solid to ultra-pure water. The FTIR spectra of three materials before and after SUL adsorption was read by a Thermo Scientific, Nicolet iS10 infrared spectrometer, USA, between 500–4000/cm bandwidth.

The proximate analysis of CWBC was carried out based on methods provided in Ahmad et al. (2013). Elemental composition (C, H, O, and N) of CWBC was estimated using an elemental analyzer (2400, Series 2 CHNS/O Analyzer, PerkinElmer). The Brunauer–Emmett–Teller (BET) surface area, pore size and volume were determined by a nitrogen adsorption analyzer (Autosorb iQ Quantachrome Instruments, USA), powder x-ray diffractogram (PXRD) was recorded to understand the crystalline nature of CWBC by powder x-ray diffractometer (XRD, Rigaku, Ultima IV, Japan), the zero-point charge of CWBC and CWBC amended soil was determined by the potentiometric titration method (HI-932, potentiometric titrator, Hanna, USA) and pH drift method described in Tran et al. (2017), respectively, and the surface

morphological orientation of CWBC was analyzed using a field emission scanning electron microscope (SEM, SU6600 FESEM; Hitachi, Japan).

2.4. pH optimization for SUL adsorption

The pH experiments were conducted using 100 mL of SUL solution (10 mg/L) with 0.01 g of CWBC and 5 g of soil or 2.5% CWBC amended soil at 298 K under N_2 gas purging environment to limit the interference of atmospheric CO_2. The initial pH of the solution was adjusted to different pH between 3–10 using NaOH (0.1 M) and HCl (0.1 M). Once the pH of the solutions was adjusted, the resulting mixtures were vigorously shaken at 150 rpm for 12 h. Finally, the mixtures were centrifuged and filtered through a 0.22 μm syringe filter to determine the equilibrium SUL concentration.

2.5. Effect of time for SUL adsorption

The kinetics of SUL adsorption on CWBC (dose: 0.1 g/L), soil (dose: 50 g/L), and 2.5% CWBC amended soil (dose: 50 g/L) was conducted at an initial SUL concentration of 10 mg/L and different times ranging from 5 to 1440 min in order to obtain the equilibrium sorption time at 298 K and pH 4.5. The solid: solution ratio was maintained similarly to the pH optimization experiment above. Finally, each mixture was centrifuged and filtered to analyze SUL equilibrium concentration.

2.6. Effect of initial strength for SUL adsorption

The adsorption effect with different initial concentrations (10–150 mg/L) on the CWBC, soil, and CWBC amended soil was investigated at pH 4.5 and 298 K at similar solid: solution ratios in the above two experiments. The resulting mixture was shaken for 12 h; the resulting solution was centrifuged and filtered to analyze equilibrium SUL concentration.

2.7. Bed column and leaching experiments

The column bed experiment was conducted in 11.5 × 3.0 cm columns made of a 50 mL syringe. The wet-filling method was followed to fill the soil and CWBC amended soil into the columns. The pore volume and porosity were determined as 20 ± 1 mL and 40 ± 2%, respectively. Initially, the columns were preconditioned and saturated with ultra-pure water (2 pore volumes) at a constant gravitational flow from top to bottom. Sequentially, a total of 13 pore volumes of 5 and 10 mg/L of SUL solutions were fed into the separate columns containing soil and CWBC amended soil. Continuously, 13 pore volume of ultra-pure water was fed in order to determine the leaching behavior of SUL through the soil and CWBC amended soil. Finally, each pore volume of solution was collected, filtered, and analyzed for the SUL concentration.

The SUL-loaded soil and CWBC amended soil of both columns were dried and used to determine the leachability by following the toxicity characteristic leaching procedure (TCLP) adopted from Vithanage et al. (2017). In brief, the soil and CWBC amended soil were mixed with a pH 4.93 buffer solution made of acetic acid and NaOH at a 1:20 w/v ratio. The resulting mixture was shaken for 18 h at 298 K. At the end, the mixture was centrifuged and filtered to determine SUL concentration.

2.8. Plant experiments

The pot experiment was conducted with soil and 2.5% CWBC amended soil in order to assess the effect of biochar in reducing the plant uptake of SUL. The addition of 2.5% woody biochar to the soil improved enzymic soil activity without affecting soil chemistry and resulted in the highest plant growth compared to the addition of 1 and 5% biochar (Bandara et al., 2017; Vithanage et al., 2018). Thus, the present study utilized 2.5% CWBC as a soil amendment to all the experiments. The *Ipomoea aquatica* plant (water spinach) seeds were purchased from Agrarian Department in Colombo, Sri Lanka. Six treatments with 2 replications were used in the pot experiment: (1) control pots with soil, A1; (2) control pots CWBC-Soil amendment, A2; (3) pots with 5 mg/kg SUL spiked soil, A3; (4) pots with 5 mg/kg SUL spiked CWBC-Soil amendment, A4; (5) pots with 50 mg/kg SUL spiked soil, A5; (6) pots with 50 mg/kg SUL spiked CWBC-Soil amendment, A6. Initially, the *Ipomoea aquatica* seeds were germinated in a germination tray until the seedlings reached 5–6 cm. The seedlings were transferred to the pots at 4 seedlings per pot. All pots were kept in a greenhouse under natural lights and environmental temperature. Once the plants grew to approximately 10 cm, the pots were spiked with SUL at 5 and 50 mg/kg. Each pot was watered two times per day with distilled water and nutrients were provided whenever necessary using Albert solution.

After 4 weeks of growth, the plants from each pot were harvested and washed several times with distilled water. The plants were separated into roots and shoots and kept in the dark environment to dry. The soil and CWBC amended soil from each pot were also kept for drying in the same manner. Once the plant materials dried, it was ground and passed through a 250 μm sieve. The ground plant materials, dried soil, and CWBC amended soil were stored at 4 °C for extraction.

2.9. The extraction of SUL from plant and soil and quantification

The extraction of SUL from the plant materials was carried out by a procedure adopted from Rajapaksha et al. (2014). In brief, 500 mg of plant material was extracted with 8 mL of 95: 5 of methanol and HCl solution by shaking the mixture for 20 min, sonicated for 10 min, centrifuged for 15 min at 4000 rpm, and the aliquot solution was collected. The remaining residue was extracted using 5 mL of acetone using the same method. Both aliquots were combined and dried with a gentle flow of N_2 gas. The residues were reconstituted with 5 mL of 50: 50 of ultra-pure water and methanol mixture. The resulting mixtures were three times de-fatted with 5 mL of hexane each time. Afterward, the remaining solutions were dried to 2.5 mL by a gentle flow of N_2 gas and passed through preconditioned SPE-HLB cartridges. Finally, the cartridges were washed a couple of times with 2.5 mL ultra-pure water each time and SUL eluted two times with 2.5 mL of methanol: acetonitrile (50: 50) each time. To the eluted solution, 40 μL of internal standard (simeton, 1 mg/L) was added and dried under the N_2 gas up to 100 μL. The final volume of solutions was increased to 400 μL by adding a diluent (0.1% formic acid in ultra-pure water and 0.1% formic acid in acetonitrile, 80: 20). In the end, the resulting solution was filtered through a 0.22 μm syringe filter.

A 5 g of Soil and CWBC amended soil from the experiment sets of A1–A6 subjected to 15 mL methanol for 20 min, sonicated for 10 min, centrifuged for 15 min at 4000 rpm, and the aliquot solution was collected (Shao et al., 2018). The remaining residue was reconstituted using 5 mL of acetone using the same method. The pooled aliquot was combined with methanol extract and dried under the gentle flow of N_2 gas at 35–40 °C until 100 μL. Finally, the resulting solution was volume up to 500 μL by adding a diluent solution and filtered through a 0.22 μm nylon syringe filter for the SUL analysis.

The SUL concentration in plant extracts was quantified using an HPLC MS/MS (Agilent 1220), while the SUL concentration in soil and CWBC amended soil was analyzed using an HPLC (Ultimate 3000, Thermo Scientific).

3. Results and discussion

3.1. CWBC characterization

Proximate and ultimate data of CWBC are tabulated in Table S1. The pH and EC of CWBC were high, at 10.8 and 494 μS/cm, respectively, possibly due to the high content of ash minerals and the pyrolysis degradation of the acidic functional groups of the feedstock. The soil pH was mildly acidic, which may be due to the decaying of soil organic

matter that yields humic substances (Ali and Mindari, 2016). Our previous study identified the soil texture as loamy sand containing kaolin clay with a cation exchange capacity of 3.8 cmol/kg (Keerthanan et al., 2021). The addition of CWBC to the soil increased the soil pH from 6.5 to 8.3, which can provide a suitable habitat for microbial growth (Rousk et al., 2010) and can alter the biochemical behavior of contaminants. Because CWBC contains 17.23% ash (Table S1), the increase in soil pH is most likely due to the release of ash constituents such as sodium, calcium, potassium, magnesium, sulfur, phosphorus, and others from the CWBC into the soil (Mukome and Parikh, 2015).

The carbon content of CWBC was 66.74% (Table S1), and was higher than *Gliricidia sepium* wood-derived biochar previously reported in Mayakaduwa et al. (2016), however, it is less than wood chips biochar derived at 700 °C in Zhu et al. (2021). Moreover, the low hydrogen content of CWBC compared to wood-based derived biochar at 500 °C (Oginni et al., 2020) indicated that there was dehydrogenation also occurred during the gasification process. The availability of polar functional groups was confirmed by the nitrogen and oxygen contents of CWBC (Table S1), which would drive the retention of SUL from the environmental matrices such as soil and water (Wu et al., 2021). Further, the low aromatic ratios (H/C *and* O/C) suggest high stability and hydrophobicity of CWBC derived at a high temperature (Yang et al., 2021).

The CWBC possessed a high surface area (589.4 m^2/g) along with 1.23 nm of mean pore radius and 0.364 cm^3/g of the total pore volume, compared to other biochars discussed in Table S2. This could be due to the further decomposition of biochar under the limited oxygen level during the gasification process (Muvhiiwa et al., 2019). The surface area of CWBC is comparatively higher than *Pinus patula* wood-derived at 700 °C reported in Rubio-Clemente et al. (2021). The volatilization and decomposition of the organic portion of cinnamon wood biomass during the gasification at a high temperature can result in a high surface area of CWBC and lead to the development of porous structure on the CWBC. The development of void structure in CWBC is further confirmed by the SEM images focused at different resolutions, as shown in Figure S1. The SEM images confirmed an ash-free heterogeneous surface formed on the CWBC surface during the gasification. The surface area and pore structure provide the number of active functional sites for the contaminant adsorption and pore filling process.

The XRD diffractogram of CWBC was shown in Figure S2a, the broadened 2θ peaks at 20°–30° described the mounting of aromatic layers in CWBC during the pyrolysis. The sharp 2θ peak at 29.4° indicated the presence of crystalline minerals such as SiO_2, in the CWBC (Freitas et al., 2020; Liu et al., 2012). The FTIR spectra of CWBC and SUL incorporated CWBC was plotted in Figure S2b. The oxygen-containing functional groups were observed in the FTIR spectrum of pristine CWBC, despite the fact that highly carbon stabilized biochar was generated during gasification, as evidenced by the high carbon content and low hydrogen content. For example, a broad frequency at 3438/cm ascribed the presence of hydroxide groups of alcoholic and phenolic compounds and a water molecule. A strong C–O stretching frequency at 1050/cm described the presence of primary alcohols on the surface of CWBC. Moreover, aromatic C–H stretching frequency at 2969/cm labeled the aromatic nature of CWBC, which was further confirmed by the aromatic C═C stretching band at 1577/cm. The peak at 1428/cm may belong to –O–H/–C–H bending vibration, further confirming oxygen-containing functional groups on the CWBC surface.

3.2. Optimization of pH for the adsorption of SUL

Fig. 1a, b, c expressed the effect of pH on the SUL adsorption onto CWBC, soil, and 2.5% of CWBC amendment, respectively. The effect of pH was investigated between pH 3–10. As shown in Fig. 1, the highest adsorption was favored at pH < 6 for all three adsorbents. A drastic decrease in adsorption capacity was observed when pH increased over 6. As discussed in Table S3, most biochars (pristine and chemically or physically modified biochar) demonstrated the maximum adsorption capacity towards SUL at pH < 6, except for base-modified biochars (Table 3S). Prasannamedha et al. (2021) reported that SUL appeared as a positively charged molecule when the pH is less than 1.7, whereas negatively charged molecule when the pH > 5.7. The pH between 1.7 and 5.7, SUL is a zwitterion. Negative and positive charged moieties on the SUL molecule formed due to the deprotonation and protonation of sulfonamide and amino group, respectively. According to Fukahori et al. (2011), SUL exists as a mixture of positive and neutral species at a pH range of 1.7–3.6 and exists as a mixture of negative and neutral species at a pH range of 3.6–5.7. On the other hand, the pHpzc of CWBC, soil, and CWBC amended soil was estimated as 7.66, 7.32, and 7.48 respectively (Figure S2c, d), and suggested that the surface charge of adsorbents is positive when solution pH is < pHpzc, whereas it is negative when the solution pH is > pHpzc (Tran et al., 2015). The maximum adsorption of SUL by CWBC, soil, and 2.5% of CWBC amended soil was observed at pH between 4 and 5.7 (Fig. 1). At this pH range, negative and neutral charged SUL molecules would have electrostatically and non-electrostatically attracted by the positively charged adsorbents (CWBC, soil, and CWBC amendment), resulting in high adsorption affinity. Above pH 5.7, there was a drastic decrease in adsorption, which may be due to the repulsive interaction between negatively charged SUL molecules and adsorbents. A similar adsorption trend SUL onto the activated carbon as a function of pH was observed in Shi et al. (2019).

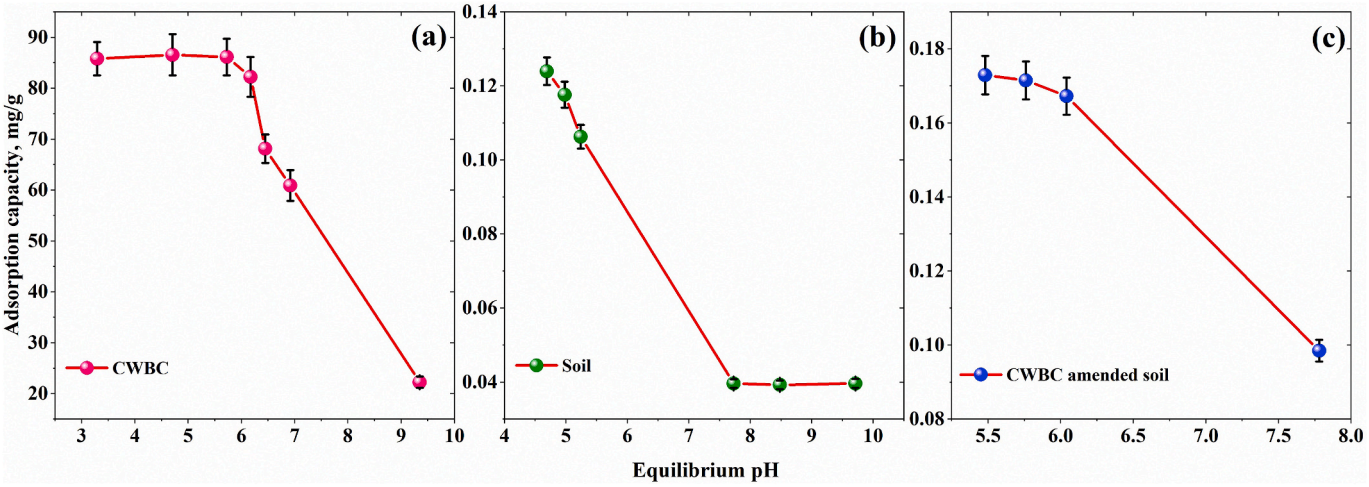

Fig. 1. The effect of pH on SUL adsorption by CWBC (a) and soil (b) and CWBC amended soil (c).

3.3. Optimization of maximum residence time

The kinetic adsorption data of SUL onto the CWBC and CWBC amended soil was well fitted with a pseudo-second-order model based on R^2 and chi^2 values, as shown in Fig. 2a and b, and the model predicted parameters are presented in Table 1. Initially, the adsorption of SUL was rapidly raised until 180 min for CWBC and 60 min for amendment and then achieved equilibrium as both systems reached the saturation points. The pseudo-second-order model predicted the maximum adsorption capacity of pristine CWBC and CWBC amended soil as 95.64 and 0.234 mg/g, respectively. These predicted values were more closely matched with the experimental values, confirming the suitability of pseudo-second-order kinetics to model the experimental data. The pseudo-second-order model accounted that SUL adsorption on CWBC and CWBC amended soil was controlled by the chemisorption process involving electrostatic attraction, hydrophobic attraction, and n–π and π–π interaction (Tang et al., 2022). In addition, multi-linear behavior patterns of adsorption capacity (q_t) as a function of $\sqrt{t}$ as shown in Fig. 2c and d elaborated that the intra-particular diffusion also played a role in the SUL removal by CWBC and CWBC amended soil (Table 1). Generally, the adsorption takes place via several processes including passage of contaminants from the bulk solution to a solid surface (film diffusion), the passage of contaminants into the pores (intra-particle diffusion), and equilibrium stage (Ben-Ali et al., 2017; Zhang et al., 2022). The diffusion model revealed that the rate governing step of SUL adsorption onto CWBC and CWBC amended soil was determined by two or more processes, including film diffusion and intra-particular diffusion, because the intercepts of plots in Fig. 2c and d are not passed through the origin. (Li et al., 2018). A similar observation was made by Zhang et al. (2022), who investigated SUL adsorption onto the boric acid-modified biochar. Further, high surface area (Table S1) and well-developed pores in CWBC (Figure S1) may provide evidence for the film diffusion and intra-particular process that took place during the adsorption of SUL in CWBC and amendment.

3.4. Optimization of maximum adsorption affinity

Fig. 3 depicts the adsorption isotherm trends of SUL onto CWBC, soil, and CWBC added to the soil. The retention of SUL in CWBC equilibrated quickly with initial concentration rises Fig. 3a, whereas it increased with SUL concentration in soil and CWBC amended soil (Fig. 3b and c). However, the retention efficiencies decreased with increasing SUL initial concentration, which might be attributed to decreasing vacant active sites on the adsorbents.

The isotherm data modeled with several non-linear regression models were displayed in Fig. 3, with the obtained parameters tabulated in Table 1. Based on the R^2 and chi^2 values, Toth isotherm and Hill isotherm models were best-matched for CWBC followed by Langmuir model, whereas Langmuir isotherm was the best-fitted model for soil and CWBC amended soil followed by Toth isotherm and Hill isotherm, in retaining of SUL (Table 1).

Generally, the Hill model assumes cooperative adsorption at the homogeneous surface of the adsorbent, where the binding energy of active sites is affected by other sites. The nature of cooperative adsorption is measured by the value of *nH* (cooperativity coefficient). The nH values 1, <1, and >1 indicate non-cooperative adsorption, negative-cooperative, and positive-cooperative adsorption process, respectively (Atugoda et al., 2020; Jayawardhana et al., 2021b). The *nH* value was 6.752, 1.017, and 0.943 for SUL retention in CWBC, soil, and amendment, respectively, suggesting that there was a positively

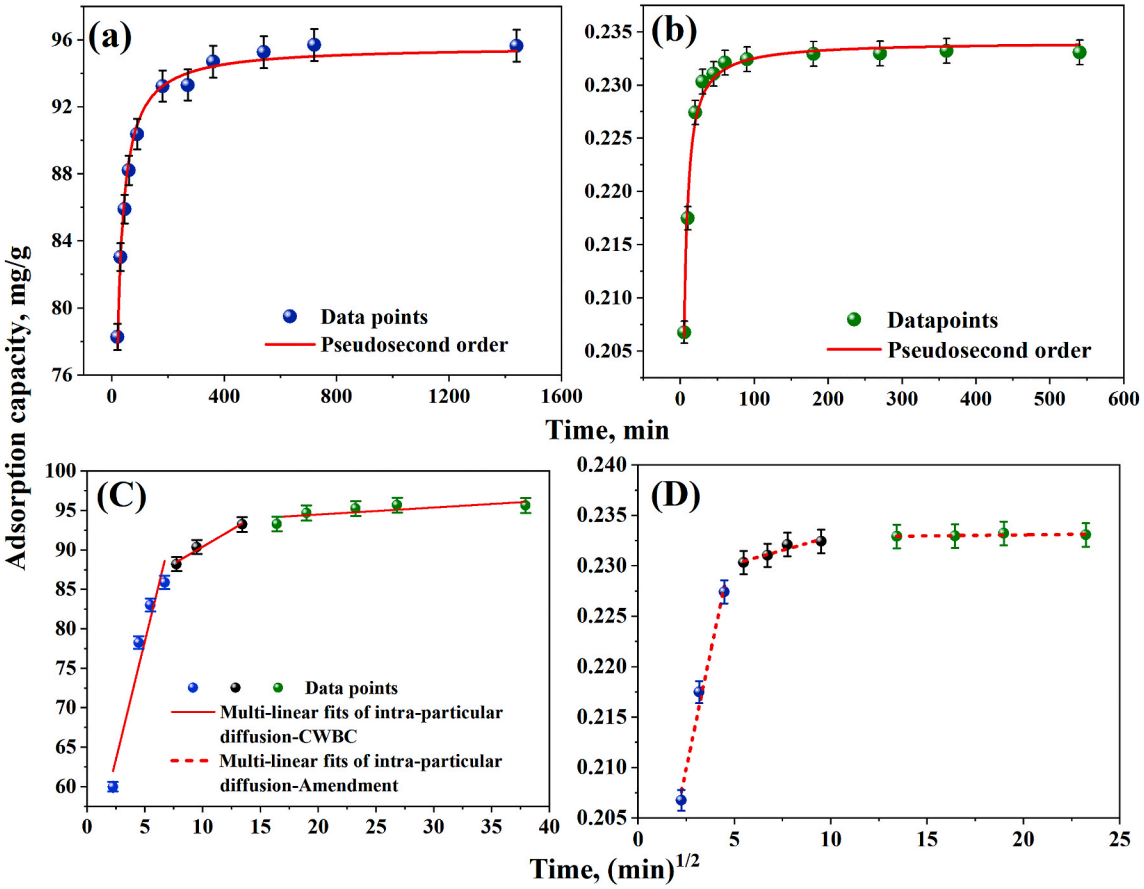

Fig. 2. The pseudo-second-order model for SUL adsorption by CWBC (a) and CWBC amended soil (b), and intra-particular diffusion for CWBC (c) and CWBC amended soil (d).

Table 1
Kinetic and isotherm models and predicted parameters.

Adsorption models	Mathematical expression		Parameters	Adsorbents		
				CWBC	Soil	2.5% CWBC amended soil
Kinetic model						
Pseudo-second-order	$q_t = \frac{(k_2\, t\, q_e^2)}{(1 + k_2\, q_e\, t)}$		k_2	0.002	–	6.363
			q_e (mg/g)	95.64		0.234
			R^2	0.991		0.989
			Chi^2	0.342		8.93E-7
Intra-particular diffusion	$q_t = k_i\sqrt{t} + C_i$ $i = 1, 2,\ and\ 3$	k_1		5.964	–	9.13E-3
		C_1		48.642		0.187
		R^2		0.943		0.985
		k_2		0.859		5.446E-4
		C_2		81.840		0.227
		R^2		0.980		0.912
		k_3		0.089		1.931E-5
		C_3		92.718		0.233
		R^2		0.581		0.345
Isotherm model						
Langmuir model (Ahmad et al., 2013)	$q_e = \frac{Q_{max} K_L C_e}{(1 + K_L C_e)}$		Q_{max} (mg/g)	118.345	0.718	3.448
			K_L	1.005	0.01	1.525
			R^2	0.764	0.949	0.989
			Chi^2	27.013	0.001	0.018
Hill model (Jakobek et al., 2020)	$q_e = \frac{Q_{max} C_e^{nH}}{K_H + C_e^{nH}}$		Q_{max} (mg/g)	113.436	0.671	3.364
			nH	6.752	1.017	0.943
			K_H	115.427	100.044	0.619
			R^2	0.991	0.947	0.972
			Chi^2	1.444	14.834	8.709
Toth model (Ghazy et al., 2021; Kumar et al., 2011)	$q_e = \frac{Q_{max} K_T C_e}{[(1 + (K_T C_e)^n]^{\frac{1}{n}}}$		Q_{max} (mg/g)	113.436	0.762	3.601
			K_T	0.296	0.009	1.955
			n	14.585	0.925	0.809
			R^2	0.991	0.947	0.974
			Chi^2	1.444	14.822	8.120

k_2: pseudo-second-order rate constant, q_e: equilibrium adsorption capacity, k_i: rate constant of intra-particle diffusion, C_i: constant related to the thickness of boundary layer, Q_{max}: maximum adsorption capacity K_L: Langmuir isotherm constant, nH: cooperativity coefficient K_H: Hill constants, K_T: Toth constant, n: Toth heterogeneity parameter.

cooperated adsorption occurred at the homogeneous surface of CWBC, whilst non-cooperative adsorption took place on the soil and CWBC amended soil since the nH is closed to unity.

Toth isotherm model is a modified form of the Langmuir model and the Toth isotherm postulates the heterogeneous adsorption of adsorbate at concentrate and dilutes concentration. The heterogeneity of adsorption is measured by the value of n (Toth heterogeneity parameter). If n is unity, then it aligns with the Langmuir model and expresses the homogeneous nature of adsorption. When n are far away from the unity, it describes the heterogeneous nature of adsorption (Ayawei et al., 2017). The n values for SUL adsorption in CWBC, soil, and CWBC amended soil were 14.585, 0.925, and 0.809, respectively, and suggested that the adsorption of SUL by CWBC ensured at heterogeneous surface. The n values for soil and CWBC amended soil were almost close to unity, suggesting that the adsorption of SUL followed the Langmuir isotherm.

Langmuir isotherm described the adsorption homogeneously distributed over the adsorbent surface and the adsorbate restricted to a monolayer on the surface at the equilibrium (Stylianou et al., 2021). Langmuir model is not found to be well fitted with SUL adsorption onto the CWBC. However, SUL adsorption by soil and CWBC amended soil followed the Langmuir model with the maximum adsorption capacity of 0.718 and 3.448 mg/g, respectively (Table 1). Further, the favorability of SUL adsorption onto soil and CWBC amended soil was determined by the Langmuir separation factor (R_L), shown in Fig. 3d. The $0 < R_L < 1$ values suggest the favorable of SUL retention by soil and amendment. The exponential decrease in R_L manifested that the adsorption of SUL became more favorable at high SUL concentration and pH 4.5. Moreover, the addition of CWBC to the soil exhibited an improvement in retaining SUL in soil.

Ultimately, the best-fitted isotherms of the Hill and Toth models for SUL by CWBC denoted that the heterogeneous and homogeneous adsorption took place with a maximum adsorption capacity of 113.436 mg/g at the experimental conditions. The homogeneous and heterogeneous surface of CWBC can be seen in the SEM images (Fig. 3). Further, the maximum retention capacity of SUL for soil and CWBC amended soil predicted by the Langmuir model demonstrated that the amendment of CWBC to soil boost the SUL retention in soil by 4.8-fold, compared to the soil.

3.5. Bed column adsorption of SUL

The transport of SUL in control soil and CWBC amended soil was investigated at environmental pH values of 6.5–8.3. The ratio between SUL concentrations in influent and effluent solution (C/C_o) was calculated at different influent SUL concentration to understand the SUL behavior in soil and CWBC amended soil, and the results are shown in Fig. 4a and b. Initially, no SUL was detected in saturated column profiles when 2 pore volumes of ultra-pure water were passed through. According to SUL behavior in the soil profile as shown in Fig. 4a, SUL was poorly retained in the soil and almost all the SUL was washed out via effluent from the soil column, whereas it was highly retained in CWBC amended soil when 13 pore volume of SUL solution and ultra-pure water were fed sequentially (Fig. 4b). The immobilized mass of SUL was determined as 2569 μg in the CWBC amended soil which accounted for 98.8% of the initially fed SUL mass. The retention of SUL in the control soil was closed to zero. The column study suggested that the application of CWBC to the soil significantly improves the SUL immobilization in soil. This observation confirmed the results of batch adsorption experiments, where the different initial condition was maintained. Similar behavior was observed in Vithanage et al. (2014), who investigated the

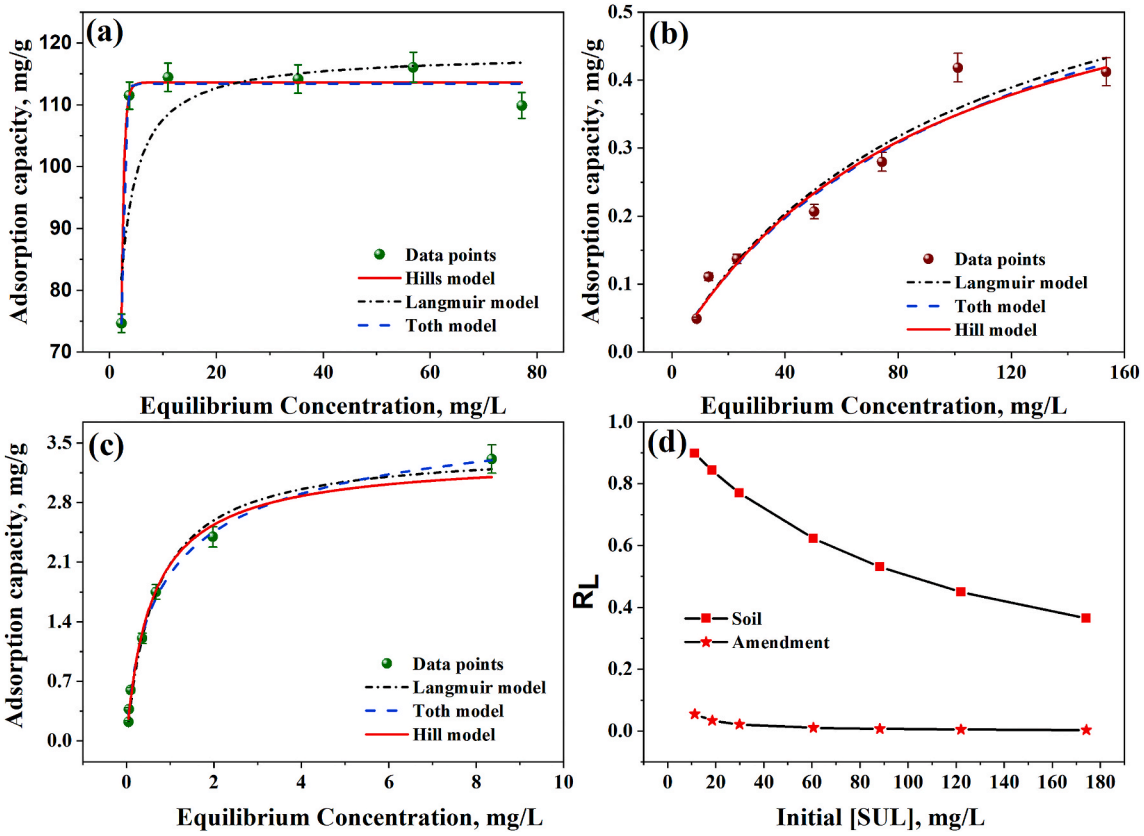

Fig. 3. Isotherm model fits for adsorption of SUL by CWBC (a), soil (b), CWBC amended soil (c), and the Langmuir model predicted separation factor (R_L) for soil and CWBC amended soil (d).

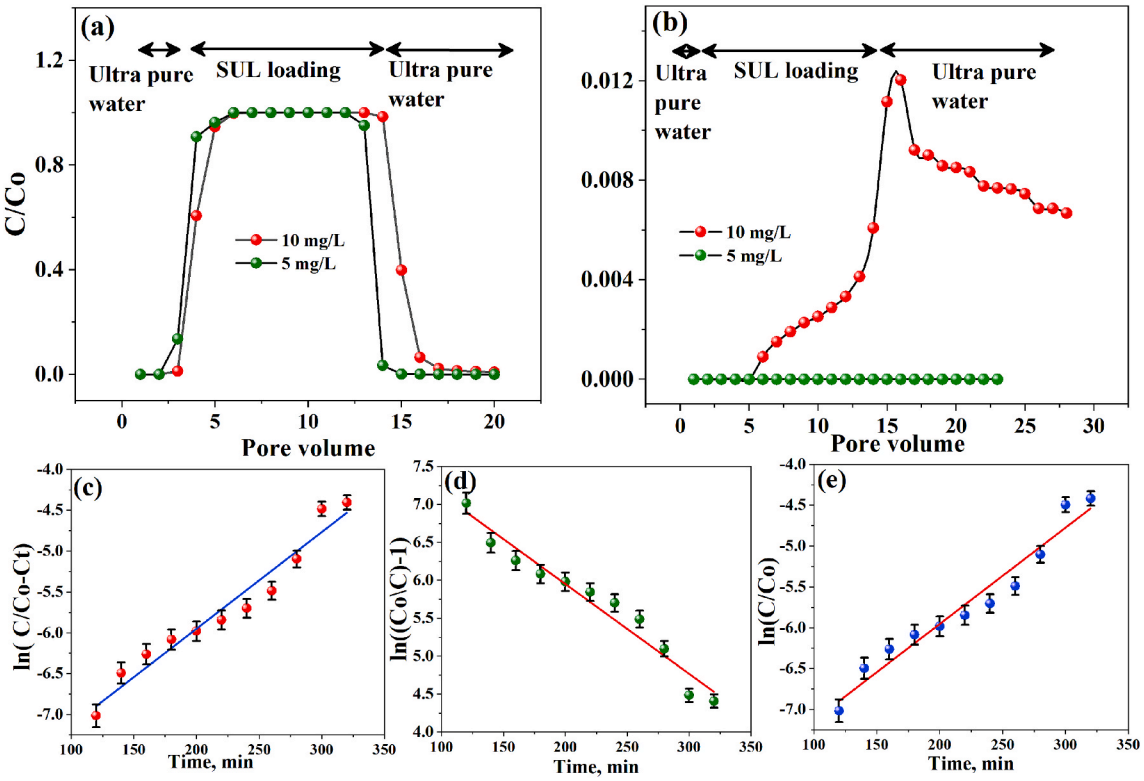

Fig. 4. Bed column breakthrough of soil (a) and CWBC amended soil (b), models of Yoon-Nelson model (c), Thomas model (d), and Adams-Bohart model (e).

immobilization of sulfamethazine through soil profile amended with invasive plant-derived biochar. Thus, CWBC can reduce the bioavailability of SUL in contaminated soil.

Further, the behavior of SUL through the CWBC amended soil was kinetically modeled with different linear models, including the Yoon-Nelson model, Thomas model, and Adams-Bohart model as shown in Fig. 4c–e, and the predicted key parameters are presented in Table 2. As per the Pearson's R, the Yoon-Nelson model and Adams-Bohart model exhibited a positive correlation (Pearson's R = 0.976) with C/C_o against time, whereas the Thomas model showed a negative correlation (Pearson's r = −0.976). The Yoon-Nelson model predicted the time (τ) taken to retain 50% of SUL on the CWBC amended soil $(C/C_o = 0.5)$ as 702.66 min in breakthrough. The maximum retention capacity predicted by the model was 0.115 mg/g, which is less than the value predicted by the adsorption kinetics model (0.234 mg/g). This may be due to the pH variation between batch adsorption study (pH ~4.5) and column adsorption (pH ~8.3). Generally, batch adsorption involves equilibrating the soil with a solution containing the SUL at a constant soil temperature and pH, whereas a solution containing the SUL is percolated down a column of soil and CWBC amended soil at a constant flow rate in bed column adsorption (Bolan et al., 1988).

Thomas model also predicted the maximum adsorption capacity as 0.115 mg/g, which is close to the value predicted by the Yoon-Nelson model, and this is in close agreement with experimentally obtained adsorption capacity at pH around 8 (Fig. 1). The second-order kinetic rate was 0.0011 L/(mg·min) and this was less than the kinetic rate predicted by the pseudo-second-order model. Thomas model assumed the adsorption is frequently limited by interphase mass transfer rather than chemical reaction kinetics (Ang et al., 2020).

Adams-Bohart model postulates that the adsorption does not occur instantly, where the adsorption rate depends on both available active sites on the adsorbent and the concentration of adsorbate. The model is used to assess the behavior of adsorbate at the early portion of breakthrough $(C/C_o < 0.15)$ (Ang et al., 2020; Chen et al., 2012). The model predicted the saturation concentration SUL as high as 10 g/L and a second-order kinetic rate of 0.0011 L/(mg·min) close to the rate predicted by the Thomas model.

3.6. Leaching of SUL

The TCLP extraction was carried out to understand the leaching behavior of SUL from the CWBC amended and unamended contaminated soil samples used in the bed column experiments. Leaching of SUL in control soil was higher than CWBC amended soil and it increased with the initial loading concentration (Figure S3). The concentration of SUL in the extract from CWBC amended soil was significantly lower than that in control soil. The addition of 2.5% of CWBC to the soil reduced the SUL in leachate by 45–49%. This could be because of the significant interaction between SUL and CWBC and intra-particular dissemination. These findings corroborated those of the adsorption batch experiment, indicating that CWBC effectively immobilized SUL in soil, thus, limiting the bioavailable fraction of SUL in soil. Similar leaching behavior of SUL was found in Tao et al. (2019), who investigated the SUL leaching from magnesium-modified biochar amended sediment.

3.7. Uptake of SUL by Ipomoea aquatica

The *Ipomoea aquatica* uptake of SUL was high in soil spiked 5 and 50 mg/kg of SUL, which may be due to the low binding ability of SUL in soil. This was confirmed with the batch experiments and column experiments. Kurade et al. (2019) observed a high accumulation of SUL in hydroponically grown *Ipomoea aquatica* in 0.05 mg/L SUL solution. Generally, SUL is accumulated more in the plant root than the shoot part due to its anionic nature. To illustrate this, the present study observed that 13.8 and 47.9 mg/kg of SUL accumulated in plant root, whereas 0.027 and 0.097 mg/kg in the shoot of *Ipomoea aquatica* grown in soil spiked with 5 and 50 mg/kg of SUL, respectively. The *Ipomoea aquatica* uptake depended on the contaminated level of SUL in soil and it increased with increasing the SUL contamination level. A previous study also indicated a higher accumulation of SUL in the root of cucumber seedling than leaf, growing in a nutrient solution for 7 days (Dudley et al., 2018). Chen et al. (2017) observed a similar trend, who exposed the *Ipomoea aquatica* and *Brassica rapa chinensis* in a cultivating solution containing 100 μg/mL SUL. In contrast, Li et al. (2020) observed a higher concentration of SUL in radish plant shoots than in roots grown in soil. This suggests that plant varieties play an important role in PPCPs uptake in plants.

3.8. Effect of CWBC amended soil in reducing plant uptake of SUL

As seen in Fig. 5, the soil concentration of SUL was increased with addition of 2.5% CWBC, which could possibly be of strong interaction between CWBC and SUL molecules. A similar observation was reported

Table 2
Bed column models and their predicted parameters for SUL adsorption for CWBC amended soil.

Models	Equations	Parameters	Predicted values
Yoon-Nelson model	$\ln\left(\frac{C}{C_o - C}\right) = K_{YN}t - \tau K_{YN}$	K_{YN} (1/min)	0.0118
		τ (min)	702.66
	$q_{YN} = \frac{\tau C_o Q}{1000M}$	q_{YN} (mg/g)	0.115
		R^2	0.952
		Pearson's R	0.976
		SS	0.312
Thomas model	$ln\left(\frac{C_o}{C} - 1\right) = \frac{k_{TH}q_{TH}M}{Q} - k_{TH}C_o t$	k_{TH} (L/mg·min)	0.0011
		q_{TH} (mg/g)	0.115
		R^2	0.952
		Pearson's R	−0.976
		SS	0.312
Adams-Bohart model	$ln\left(\frac{C}{C_o}\right) = K_{AB}C_o t - \frac{K_{AB}N_o z}{U_o}$	K_{AB} (L/mg·min)	0.0011
		N_o (mg/L)	10063.73
		R^2	0.952
		Pearson's R	0.976
		SS	0.307

K_{YN}: Yoon-Nelson rate constant, τ: time taken to retain 50% of SUL in bed column, q_{YN}: Yoon-Nelson maximum adsorption capacity, k_{TH}: Thomas rate constant, q_{TH}: Thomas uptake capacity, M: mass of soil packed in columns, Q/U_o: linear flow rate of SUL solution through the columns, K_{AB}: Bohart-Adams rate constant, N_o: uptake volumetric capacity, z: height of column, SS: residual sum of squares.

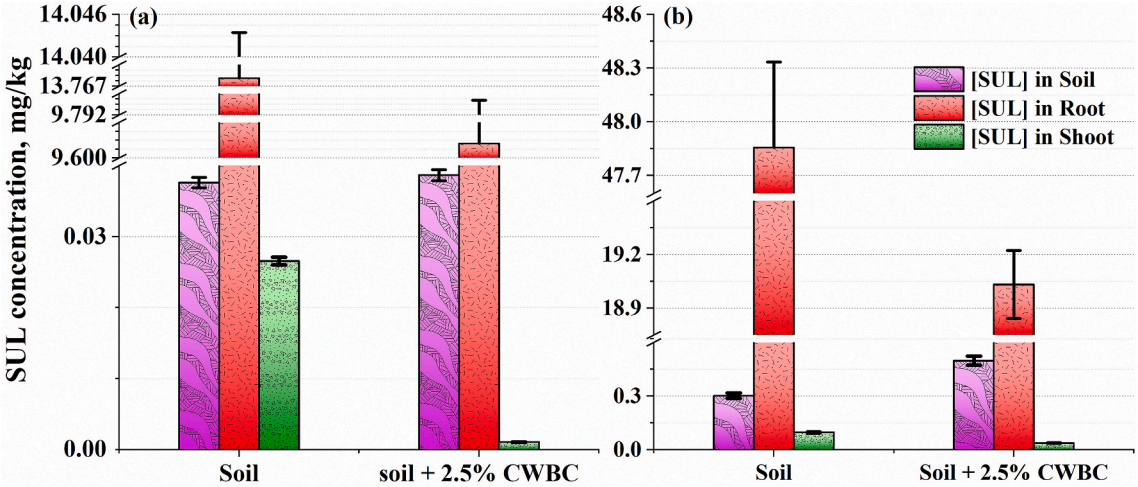

Fig. 5. Plant uptake of SUL in soil and CWBC amended soil at different spiked rate of 5 mg/kg (a) and 50 mg/kg (b).

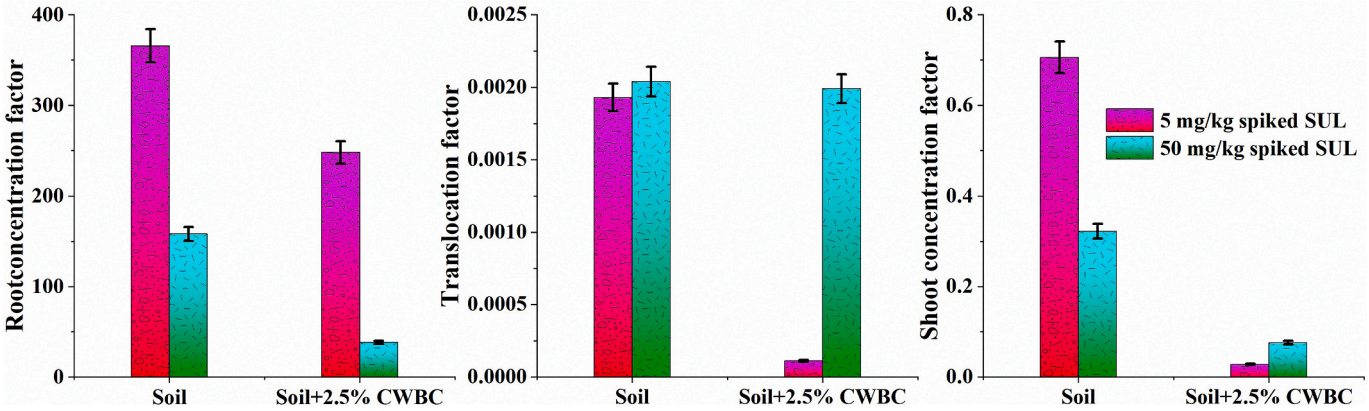

Fig. 6. Plant accumulation factors of SUL grown in soil and CWBC amended soil spiked with different concentration of SUL: *Rootconcentration factor* $= \frac{[SUL]root}{[SUL]soil/amendment}$, *Translocation factor* $= \frac{[SUL]shoot}{[SUL]root}$, and *Shoot concentration factor* $= \frac{[SUL]shoot}{[SUL]soil/amendment}$

in Hurtado et al. (2017), who investigated the effect of woody biochar in plant uptake of PPCPs, including triclosan, caffeine, ibuprofen, etc. The addition of 2.5% CWBC to the soil potentially reduced the plant uptake of SUL from the contaminated soil (Fig. 5), possibly because the CWBC reduced the bioavailable portion of SUL by strongly binding with it (Rajapaksha et al., 2014) and the possible SUL adsorptive mechanism was proposed in Figure S4 of supplementary document. The CWBC amended soil decreased the SUL accumulation in the root by 30 and 60% and shoot by 95 and 61% of *Ipomoea aquatica* in a CWBC amended soil treated with 5 and 50 mg/kg SUL, respectively. This is in line with prior research that found significant reductions in plant uptake of PPCPs by amending soil with wood-derived biochar (Hurtado et al., 2017; Li et al., 2020; You et al., 2020).

3.9. Effect of biochar on bioaccumulation factors (BCF) of SUL

The root concentration factor (RCF), translocation factor (TF), and shoot concentration factor (SCF) in soil and CWBC amended soil were plotted in Fig. 6. The RCF of SUL in *Ipomoea aquatica* was higher than TF and BCF. Generally, the anionic PPCPs such as SUL penetrate into the root cells with water and accumulate there, probably due to repulsion by negatively charged cell walls (Goldstein et al., 2014). The addition of 2.5% of CWBC to the soil diminished the RCF, TF, and SCF by 32.14, 94.17, and 96.05%, respectively, when growing media spiked with 5 mg/kg SUL. Similarly, it was reduced by 75.89, 2.42, and 76.47%, respectively when 50 mg/kg SUL spiked to the CWBC amended soil. The 2.5% CWBC amended soil significantly decreased ($p < 0.05$) the RCF, TF, and SCF when spiked with 5 mg/kg SUL. However, it is not significantly reduced ($p > 0.05$) the factors when the grown media was contaminated with 50 mg/kg SUL.

The relative bioconcentration factors (RBF) of SUL in shoot and root of *Ipomoea aquatica* was calculated by using Equation S6 at both high (50 mg/kg) and low (5 mg/kg) SUL application rate (Figure S5). The RBF for SUL in shoot and root of *Ipomoea aquatica* at both low and high spiked rate, decreased <1 with the addition of 2.5% CWBC to the soil. Strong interactions between SUL and CWBC may be responsible for this behavior, as explained in Figure S4.

4. Conclusion

The CWBC obtained from the energy generating industry had a high porous character, resulting in a large surface area (589.4 m^2/g). The SUL affinity towards CWBC was strong (113.4 mg/g) and pH-sensitive. The findings of the batch sorption, bed column, and leaching experiments indicated that SUL has high bioavailability in soil due to its poor adsorption affinity, and hence SUL is significantly mobilized in the soil. The uptake of SUL by *Ipomoea aquatica* was high and was dependent on the level of SUL contamination in the soil. When soil was spiked with 5 and 50 mg/kg, SUL accumulation in the plant was 9.6–13.8 and 19.1–48 mg/kg respectively, indicating that the *Ipomoea aquatica* has a high capacity for SUL uptake. The amount of SUL accumulated in the root was much higher (9.6–47.9 mg/kg) than in the shoot (0.001–0.1 mg/kg).

The Hill isotherm model and bed column adsorption suggested that the adding 2.5% CWBC to the soil improved SUL soil adsorption from 0.67 to 3.36 mg/g and 98.8% retention from initially loaded SUL, resulting in 30–60% reduction in root accumulation and 61–95% reduction in shoot accumulation due to limiting the bioavailable fraction of SUL in soil. The present study suggests using CWBC to minimize the bioavailable portion of SUL for plant uptake in soil. However, the current investigation was conducted on a laboratory scale to determine the efficacy of CWBC in restricting SUL fate in the environment. As a result, more research has to be conducted in realistic agricultural land with biochar application. Furthermore, the metabolic modification of SUL in the environment is a significant element that can affect SUL's toxicity to the environment and living beings. This is something that needs to be looked at more. And, the catalytic removal of SUL by CWBC also needs to be investigated in future research.

Credit author statement

S. Keerthanan: Experimentation, data interpretation, data validation, writing the first draft; **Chamila Jayasinghe**: Supervision, Funding acquisition, Reviewing and editing; **Nanthi Bolan**: Writing-reviewing and editing; **Jorg Rinklebe**: Writing-reviewing and editing; **Meththika Vithanage**: Conceptualization, supervision, project administration, funding acquisition, writing-reviewing and editing.

Declaration of competing interest

The authors declare that they have no known competing financial interests or personal relationships that could have appeared to influence the work reported in this paper.

Acknowledgments

Authors acknowledge financial assistant (Grant No: ASP/01/RE/SCI/2018–65) provided by the Research Council, University of Sri Jayewardenepura, Sri Lanka.

Appendix A. Supplementary data

Supplementary data to this article can be found online at https://doi.org/10.1016/j.chemosphere.2022.134073.

References

Ahmad, M., Lee, S.S., Rajapaksha, A.U., Vithanage, M., Zhang, M., Cho, J.S., Lee, S.-E., Ok, Y.S., 2013. Trichloroethylene adsorption by pine needle biochars produced at various pyrolysis temperatures. Bioresour. Technol. 143, 615–622.

Ali, M., Mindari, W., 2016. Effect of Humic Acid on Soil Chemical and Physical Characteristics of Embankment. EDP Sciences, p. 1028.

Ang, T.N., Young, B.R., Taylor, M., Burrell, R., Aroua, M.K., Baroutian, S.J.C., 2020. Breakthrough Analysis of Continuous Fixed-Bed Adsorption of Sevoflurane Using Activated Carbons, vol. 239, p. 124839.

Ashiq, A., Adassooriya, N.M., Sarkar, B., Rajapaksha, A.U., Ok, Y.S., Vithanage, M., 2019. Municipal solid waste biochar-bentonite composite for the removal of antibiotic ciprofloxacin from aqueous media. J. Environ. Manag. 236, 428–435.

Atugoda, T., Wijesekara, H., Werellagama, D.R.I.B., Jinadasa, K.B.S.N., Bolan, N.S., Vithanage, M., 2020. Adsorptive interaction of antibiotic ciprofloxacin on polyethylene microplastics: implications for vector transport in water. Environ. Technol. Innovat. 19, 100971, 100971.

Ayawei, N., Ebelegi, A.N., Wankasi, D., 2017. Modelling and interpretation of adsorption isotherms. J. Chem. 2017, 3039817.

Azanu, D., Styrishave, B., Darko, G., Weisser, J.J., Abaidoo, R.C., 2018. Occurrence and risk assessment of antibiotics in water and lettuce in Ghana. Sci. Total Environ. 622–623, 293–305.

Bandara, T., Herath, I., Kumarathilaka, P., Seneviratne, M., Seneviratne, G., Rajakaruna, N., Vithanage, M., Ok, Y.S., 2017. Role of woody biochar and fungal-bacterial co-inoculation on enzyme activity and metal immobilization in serpentine soil. J. Soils Sediments 17 (3), 665–673.

Ben-Ali, S., Jaouali, I., Souissi-Najar, S., Ouederni, A., 2017. Characterization and adsorption capacity of raw pomegranate peel biosorbent for copper removal. J. Clean. Prod. 142, 3809–3821.

Bolan, N.S., Syers, J.K., Tillman, R.W., 1988. Effect of pH on the adsorption of phosphate and potassium in batch and in column experiments. Soil Res. 26 (1), 165–170.

Cao, Y., Yang, B., Song, Z., Wang, H., He, F., Han, X., 2016. Wheat straw biochar amendments on the removal of polycyclic aromatic hydrocarbons (PAHs) in contaminated soil. Ecotoxicol. Environ. Saf. 130, 248–255.

Chen, Hui-Ru, Rairat, Tirawat, Loh, Shih-Hurng, Wu, Yu-Chieh, Vickroy, Thomas W., Chou, Chi-Chung, 2017. Assessment of veterinary drugs in plants using pharmacokinetic approaches: The absorption, distribution and elimination of tetracycline and sulfamethoxazole in ephemeral vegetables. PLOS ONE 12 (8), e0183087. https://doi.org/10.1371/journal.pone.0183087.

Chen, S., Yue, Q., Gao, B., Li, Q., Xu, X., Fu, K., 2012. Adsorption of hexavalent chromium from aqueous solution by modified corn stalk: a fixed-bed column study. Bioresour. Technol. 113, 114–120.

Christou, A., Karaolia, P., Hapeshi, E., Michael, C., Fatta-Kassinos, D., 2017. Long-term wastewater irrigation of vegetables in real agricultural systems: concentration of pharmaceuticals in soil, uptake and bioaccumulation in tomato fruits and human health risk assessment. Water Res. 109, 24–34.

Dudley, S., Sun, C., Jiang, J., Gan, J., 2018. Metabolism of sulfamethoxazole in Arabidopsis thaliana cells and cucumber seedlings. Environ. Pollut. 242, 1748–1757.

Ferrari, B., Mons, R., Vollat, B., Fraysse, B., Paxēaus, N., Giudice, R.L., Pollio, A., Garric, J., 2004. Environmental risk assessment of six human pharmaceuticals: are the current environmental risk assessment procedures sufficient for the protection of the aquatic environment? Environ. Toxicol. Chem. 23 (5), 1344–1354.

Freitas, A.M., Nair, V.D., Harris, W.G., 2020. Biochar as influenced by feedstock variability: implications and opportunities for phosphorus management. Front. Sustain. Food Syst. 4, 150.

Fukahori, S., Fujiwara, T., Ito, R., Funamizu, N., 2011. pH-Dependent adsorption of sulfa drugs on high silica zeolite: modeling and kinetic study. Desalination 275 (1), 237–242.

Ghazy, M., Askalany, A., Kamel, A., Khalil, K.M.S., Mohammed, R.H., Saha, B.B., 2021. Performance enhancement of adsorption cooling cycle by pyrolysis of Maxsorb III activated carbon with ammonium carbonate. Int. J. Refrig. 126, 210–221.

Goldstein, M., Shenker, M., Chefetz, B., 2014. Insights into the uptake processes of wastewater-borne pharmaceuticals by vegetables. Environ. Sci. Technol. 48 (10), 5593–5600.

Guruge, K.S., Goswami, P., Tanoue, R., Nomiyama, K., Wijesekara, R.G.S., Dharmaratne, T.S., 2019. First nationwide investigation and environmental risk assessment of 72 pharmaceuticals and personal care products from Sri Lankan surface waterways. Sci. Total Environ. 690, 683–695.

Hassan, M., Liu, Y., Naidu, R., Du, J., Qi, F., 2020. Adsorption of Perfluorooctane sulfonate (PFOS) onto metal oxides modified biochar. Environ. Technol. Innovat. 19, 100816.

He, K., He, G., Wang, C., Zhang, H., Xu, Y., Wang, S., Kong, Y., Zhou, G., Hu, R., 2020. Biochar amendment ameliorates soil properties and promotes Miscanthus growth in a coastal saline-alkali soil. Appl. Soil Ecol. 155, 103674.

Hurtado, C., Cañameras, N., Domínguez, C., Price, G.W., Comas, J., Bayona, J.M., 2017. Effect of soil biochar concentration on the mitigation of emerging organic contaminant uptake in lettuce. J. Hazard Mater. 323, 386–393.

Isidori, M., Lavorgna, M., Nardelli, A., Pascarella, L., Parrella, A., 2005. Toxic and genotoxic evaluation of six antibiotics on non-target organisms. Sci. Total Environ. 346 (1), 87–98.

Jakobek, L., Matić, P., Kraljević, Š., Ukić, Š., Benšić, M., Barron, A.R., 2020. Adsorption between Quercetin Derivatives and β-Glucan Studied with a Novel Approach to Modeling Adsorption Isotherms, vol. 10, p. 1637, 5.

Jayawardhana, Y., Keerthanan, S., Lam, S.S., Vithanage, M., 2021a. Ethylbenzene and toluene interactions with biochar from municipal solid waste in single and dual systems. Environ. Res. 197 (October 2020), 111102, 111102.

Jayawardhana, Y., Keerthanan, S., Lam, S.S., Vithanage, M., 2021b. Ethylbenzene and toluene interactions with biochar from municipal solid waste in single and dual systems. Environ. Res. 197, 111102.

Keerthanan, S., Gunawardane, C., Somasundaram, T., Jayampathi, T., Jayasinghe, C., Vithanage, M., 2021. Immobilization and retention of caffeine in soil amended with Ulva reticulata biochar. J. Environ. Manag. 281, 111852.

Kumar, K.V., Monteiro de Castro, M., Martinez-Escandell, M., Molina-Sabio, M., Rodriguez-Reinoso, F., 2011. A site energy distribution function from Toth isotherm for adsorption of gases on heterogeneous surfaces. Phys. Chem. Chem. Phys. 13 (13), 5753–5759.

Kurade, M.B., Xiong, J.-Q., Govindwar, S.P., Roh, H.-S., Saratale, G.D., Jeon, B.-H., Lim, H., 2019. Uptake and biodegradation of emerging contaminant sulfamethoxazole from aqueous phase using Ipomoea aquatica. Chemosphere 225, 696–704.

Li, J., Yu, G., Pan, L., Li, C., You, F., Xie, S., Wang, Y., Ma, J., Shang, X., 2018. Study of ciprofloxacin removal by biochar obtained from used tea leaves. J. Environ. Sci. (China) 73, 20–30.

Li, Y., He, J., Qi, H., Li, H., Boyd, S.A., Zhang, W., 2020. Impact of biochar amendment on the uptake, fate and bioavailability of pharmaceuticals in soil-radish systems. J. Hazard Mater. 398, 122852.

Liu, X., Liang, C., Liu, X., Zhao, F., Han, C., 2020. Occurrence and human health risk assessment of pharmaceuticals and personal care products in real agricultural systems with long-term reclaimed wastewater irrigation in Beijing, China. Ecotoxicol. Environ. Saf. 190, 110022.

Liu, Y., Zhao, X., Li, J., Ma, D., Han, R., 2012. Characterization of bio-char from pyrolysis of wheat straw and its evaluation on methylene blue adsorption. Desalination Water Treat. 46 (1–3), 115–123.

Mayakaduwa, S.S., Kumarathilaka, P., Herath, I., Ahmad, M., Al-Wabel, M., Ok, Y.S., Usman, A., Abduljabbar, A., Vithanage, M., 2016. Equilibrium and kinetic

mechanisms of woody biochar on aqueous glyphosate removal. Chemosphere 144, 2516–2521.
Mukome, F.N.D., Parikh, S.J., Yong Sik, Ok, S M U, Chang, Scott X., 2015. Biochar Production. In: Bolan, Nanthi (Ed.), Characterization, and Applications. CRC Press, Boca Raton, FL.
Muvhiiwa, R., Kuvarega, A., Llana, E.M., Muleja, A., 2019. Study of biochar from pyrolysis and gasification of wood pellets in a nitrogen plasma reactor for design of biomass processes. J. Environ. Chem. Eng. 7 (5), 103391.
Oginni, O., Yakaboylu, G.A., Singh, K., Sabolsky, E.M., Unal-Tosun, G., Jaisi, D., Khanal, S., Shah, A., 2020. Phosphorus adsorption behaviors of MgO modified biochars derived from waste woody biomass resources. J. Environ. Chem. Eng. 8 (2), 103723.
Panwar, N.L., Pawar, A., Salvi, B.L., 2019. Comprehensive review on production and utilization of biochar. SN Appl. Sci. 1 (2), 168.
Plaimart, J., Acharya, K., Mrozik, W., Davenport, R.J., Vinitnantharat, S., Werner, D., 2021. Coconut husk biochar amendment enhances nutrient retention by suppressing nitrification in agricultural soil following anaerobic digestate application. Environ. Pollut. 268, 115684.
Prasannamedha, G., Kumar, P.S., Mehala, R., Sharumitha, T.J., Surendhar, D., 2021. Enhanced adsorptive removal of sulfamethoxazole from water using biochar derived from hydrothermal carbonization of sugarcane bagasse. J. Hazard Mater. 407, 124825.
Rajapaksha, A.U., Vithanage, M., Lim, J.E., Ahmed, M.B.M., Zhang, M., Lee, S.S., Ok, Y. S., 2014. Invasive plant-derived biochar inhibits sulfamethazine uptake by lettuce in soil. Chemosphere 111, 500–504.
Rousk, J., Bååth, E., Brookes, P.C., Lauber, C.L., Lozupone, C., Caporaso, J.G., Knight, R., Fierer, N., 2010. Soil bacterial and fungal communities across a pH gradient in an arable soil. ISME J. 4 (10), 1340–1351.
Rubio-Clemente, A., Gutiérrez, J., Henao, H., Melo, A.M., Pérez, J.F., Chica, E., 2021. Adsorption Capacity of the Biochar Obtained from Pinus Patula Wood Micro-gasification for the Treatment of Polluted Water Containing Malachite Green Dye. Journal of King Saud University - Engineering Sciences.
Scholar, E., 2007. In: Enna, S.J., Bylund, D.B. (Eds.), xPharm: the Comprehensive Pharmacology Reference. Elsevier, New York, pp. 1–5.
Shan, R., Shi, Y., Gu, J., Wang, Y., Yuan, H., 2020. Single and competitive adsorption affinity of heavy metals toward peanut shell-derived biochar and its mechanisms in aqueous systems. Chin. J. Chem. Eng. 28 (5), 1375–1383.
Shao, Y., Yang, K., Jia, R., Tian, C., Zhu, Y., 2018. Degradation of triclosan and carbamazepine in two agricultural and garden soils with different textures amended with composted sewage sludge. Int. J. Environ. Res. Publ. Health 15 (11).
Shi, Y., Liu, G., Wang, L., Zhang, H., 2019. Activated carbons derived from hydrothermal impregnation of sucrose with phosphoric acid: remarkable adsorbents for sulfamethoxazole removal. RSC Adv. 9 (31), 17841–17851.
Sivagami, K., Vignesh, V.J., Srinivasan, R., Divyapriya, G., Nambi, I.M., 2020. Antibiotic usage, residues and resistance genes from food animals to human and environment: an Indian scenario. J. Environ. Chem. Eng. 8 (1), 102221.
Straub, J.O., 2016. Aquatic environmental risk assessment for human use of the old antibiotic sulfamethoxazole in Europe. Environ. Toxicol. Chem. 35 (4), 767–779.
Stylianou, M., Christou, A., Michael, C., Agapiou, A., Papanastasiou, P., Fatta-Kassinos, D., 2021. Adsorption and removal of seven antibiotic compounds present in water with the use of biochar derived from the pyrolysis of organic waste feedstocks. J. Environ. Chem. Eng. 9 (5), 105868.
Sun, C., Dong, D., He, S., Zhang, L., Zhang, X., Wang, C., Hua, X., Guo, Z., 2019. Multimedia fate modeling of antibiotic sulfamethoxazole, lincomycin, and florfenicol in a seasonally ice-covered river receiving WWTP effluents. Environ. Sci. Pollut. Control Ser. 26 (17), 17351–17361.
Sun, C., Dudley, S., Trumble, J., Gan, J., 2018. Pharmaceutical and personal care products-induced stress symptoms and detoxification mechanisms in cucumber plants. Environ. Pollut. 234, 39–47.
Tang, Y., Li, Y., Zhan, L., Wu, D., Zhang, S., Pang, R., Xie, B., 2022. Removal of emerging contaminants (bisphenol A and antibiotics) from kitchen wastewater by alkali-modified biochar. Sci. Total Environ. 805, 150158.
Tao, Q., Li, B., Li, Q., Han, X., Jiang, Y., Jupa, R., Wang, C., Li, T., 2019. Simultaneous remediation of sediments contaminated with sulfamethoxazole and cadmium using magnesium-modified biochar derived from Thalia dealbata. Sci. Total Environ. 659, 1448–1456.
Tran, H.N., Wang, Y.-F., You, S.-J., Chao, H.-P., 2017. Insights into the mechanism of cationic dye adsorption on activated charcoal: the importance of π–π interactions. Process Saf. Environ. Protect. 107, 168–180.
Tran, H.N., You, S.-J., Chao, H.-P., 2015. Effect of pyrolysis temperatures and times on the adsorption of cadmium onto orange peel derived biochar. Waste Manag. Res. 34 (2), 129–138.
Uchimiya, M., Lima, I.M., Klasson, K.T., Wartelle, L.H., 2010. Contaminant immobilization and nutrient release by biochar soil amendment: roles of natural organic matter. Chemosphere 80 (8), 935–940.
Vithanage, M., Bandara, T., Al-Wabel, M.I., Abduljabbar, A., Usman, A.R.A., Ahmad, M., Ok, Y.S., 2018. Soil enzyme activities in waste biochar amended multi-metal contaminated soil; effect of different pyrolysis temperatures and application rates. Commun. Soil Sci. Plant Anal. 49 (5), 635–643.
Vithanage, M., Herath, I., Almaroai, Y.A., Rajapaksha, A.U., Huang, L., Sung, J.-K., Lee, S.S., Ok, Y.S., 2017. Effects of carbon nanotube and biochar on bioavailability of Pb, Cu and Sb in multi-metal contaminated soil. Environ. Geochem. Health 39 (6), 1409–1420.
Vithanage, M., Rajapaksha, A.U., Tang, X., Thiele-Bruhn, S., Kim, K.H., Lee, S.-E., Ok, Y. S., 2014. Sorption and transport of sulfamethazine in agricultural soils amended with invasive-plant-derived biochar. J. Environ. Manag. 141, 95–103.
Wu, Y., Cheng, H., Pan, D., Zhang, L., Li, W., Song, Y., Bian, Y., Jiang, X., Han, J., 2021. Potassium hydroxide-modified algae-based biochar for the removal of sulfamethoxazole: sorption performance and mechanisms. J. Environ. Manag. 293, 112912.
Yang, J., Gao, X., Li, J., Zuo, R., Wang, J., Song, L., 2021. The distribution and speciation characteristics of vanadium in typical cultivated soils. Int. J. Environ. Anal. Chem. 1–14.
You, X., Jiang, H., Zhao, M., Suo, F., Zhang, C., Zheng, H., Sun, K., Zhang, G., Li, F., Li, Y., 2020. Biochar reduced Chinese chive (Allium tuberosum) uptake and dissipation of thiamethoxam in an agricultural soil. J. Hazard Mater. 390, 121749.
Zhang, M., Zhang, L., Riaz, M., Xia, H., Jiang, C., 2021. Biochar amendment improved fruit quality and soil properties and microbial communities at different depths in citrus production. J. Clean. Prod. 292, 126062.
Zhang, X., Gang, D.D., Zhang, J., Lei, X., Lian, Q., Holmes, W.E., Zappi, M.E., Yao, H., 2022. Insight into the activation mechanisms of biochar by boric acid and its application for the removal of sulfamethoxazole. J. Hazard Mater. 424, 127333.
Zhang, Y.P., Adi, V.S.K., Huang, H.-L., Lin, H.-P., Huang, Z.-H., 2019. Adsorption of metal ions with biochars derived from biomass wastes in a fixed column: adsorption isotherm and process simulation. J. Ind. Eng. Chem. 76, 240–244.
Zhu, H., Liu, X., Jiang, Y., Zhang, M., Lin, D., Yang, K., 2021. Time-dependent desorption of anilines, phenols, and nitrobenzenes from biochar produced at 700 °C: insight into desorption hysteresis. Chem. Eng. J. 422, 130584.